Received: 5 July 2017 | Accepted: 4 August 2017

DOI: 10.1111/gcb.13875

PRIMARY RESEARCH ARTICLE

WILEY Global Change Biology

Tracing biogeochemical subsidies from glacier runoff into Alaska's coastal marine food webs

Mayumi L. Arimitsu[1] | Keith A. Hobson[2] | D'Arcy N. Webber[3] | John F. Piatt[4] | Eran W. Hood[5] | Jason B. Fellman[5]

[1]U.S. Geological Survey Alaska Science Center, Juneau, AK, USA

[2]Environment and Climate Change Canada, Saskatoon, SK, Canada

[3]Quantifish, Hairini, Tauranga, New Zealand

[4]U.S. Geological Survey Alaska Science Center, Anchorage, AK, USA

[5]University of Alaska Southeast, Juneau, AK, USA

Correspondence
Mayumi L. Arimitsu, U.S. Geological Survey Alaska Science Center, Juneau, AK, USA.
Email: marimitsu@usgs.gov

Funding information
North Pacific Research Board, Grant/Award Number: 1206

Abstract

Nearly half of the freshwater discharge into the Gulf of Alaska originates from landscapes draining glacier runoff, but the influence of the influx of riverine organic matter on the trophodynamics of coastal marine food webs is not well understood. We quantified the ecological impact of riverine organic matter subsidies to glacier-marine habitats by developing a multi-trophic level Bayesian three-isotope mixing model. We utilized large gradients in stable ($\delta^{13}C$, $\delta^{15}N$, $\delta^{2}H$) and radiogenic ($\Delta^{14}C$) isotopes that trace riverine and marine organic matter sources as they are passed from lower to higher trophic levels in glacial-marine habitats. We also compared isotope ratios between glacial-marine and more oceanic habitats. Based on isotopic measurements of potential baseline sources, ambient water and tissues of marine consumers, estimates of the riverine organic matter source contribution to upper trophic-level species including fish and seabirds ranged from 12% to 44%. Variability in resource use among similar taxa corresponded to variation in species distribution and life histories. For example, riverine organic matter assimilation by the glacier-nesting seabirds Kittlitz's murrelet (*Brachyramphus brevirostris*) was greater than that of the forest-nesting marbled murrelet (*B. marmoratus*). The particulate and dissolved organic carbon in glacial runoff and near surface coastal waters was aged (12100–1500 years BP ^{14}C-age) but dissolved inorganic carbon and biota in coastal waters were young (530 years BP ^{14}C-age to modern). Thus terrestrial-derived subsidies in marine food webs were primarily composed of young organic matter sources released from glacier ecosystems and their surrounding watersheds. Stable isotope compositions also revealed a divergence in food web structure between glacial-marine and oceanic sites. This work demonstrates linkages between terrestrial and marine ecosystems, and facilitates a greater understanding of how climate-driven changes in freshwater runoff have the potential to alter food web dynamics within coastal marine ecosystems in Alaska.

KEYWORDS
$\delta^{13}C$, $\delta^{15}N$ $\Delta^{14}C$, $\delta^{2}H$, Bayesian isotope mixing model, glacier runoff, marine ecosystem, marine food web

1 | INTRODUCTION

Rates of glacier mass loss in Alaska over recent decades (75 ± 11 Gt/year between 1994 and 2013) are among the highest on Earth (Larsen et al., 2015). Glacial runoff (water and ice discharged from glaciers and icefields) accounts for nearly half of all freshwater discharge into the Gulf of Alaska (Neal, Hood, & Smikrud, 2010). Freshwater is a driver of the Alaska Coastal Current, a prominent nearshore circulation feature that can be traced from the Gulf of Alaska through passes in the Aleutian Islands into the Bering Sea and Arctic Ocean by its low salinity signature (Weingartner, Danielson, & Royer, 2005). Rates of glacier mass loss in the region increased in recent decades (Arendt, Walsh, & Harrison, 2009), however, with continued glacier wastage meltwater discharge is projected to decrease 20% by the end of the century (Bliss, Hock, & Radić, 2014). Changes of this magnitude may have important implications for the physical and biogeochemical properties of downstream marine ecosystems.

The trophic ecology of glacial-marine food webs is influenced by glacier runoff driven habitat gradients (Arimitsu, Piatt, & Mueter, 2016). Within the turbid plume near tidewater glaciers, suspended glacial silt restricts light to the water column, limits phytoplankton biomass (Piwosz et al., 2009) and inhibits the diel vertical migration behavior of the typical mesopelagic species. For example, krill and plankton-feeding fish that typically occur in deep water during light hours are abundant in near-surface glacier plume waters during the day (Abookire, Piatt, & Speckman, 2002; Arimitsu, Piatt, Madison, Conaway, & Hillgruber, 2012). Cold-water forage fish spawn in glacial fjords that provide thermal refuge from warmer ocean temperatures (Arimitsu et al., 2008). Surface-feeding seabird predators exploit shallow prey upwelled by tidewater fjord circulation and ice calving events (Lydersen et al., 2014), and other seabirds use these areas, in part, because of proximity to their glacial nesting habitat (Kissling, Lukacs, Gende, & Lewis, 2015).

During peak melt season in summer, glacial-marine food webs may lack the high-quality autotrophic biomass needed to fuel them (Vargas et al., 2011). Although riverine systems typically have much lower levels of primary productivity than coastal marine systems (Hedges, Keil, & Benner, 1997), riverine organic matter (OM) subsidies in glacial-marine food webs may be important because of low in situ primary productivity where light penetration is restricted by glacial silt (Piwosz et al., 2009). Thus allochthonous subsidies may be important for stabilizing these food webs where availability of local resources is limited or variable (Batt et al., 2015).

The riverine OM carried in glacier runoff is a mixture of terrigenous OM from land plants, aquatic microbial OM and glacier-derived OM (Fellman et al., 2015), all of which are produced in environments dominated by ambient freshwater. As a result, riverine OM has a unique $^{2}H/^{1}H$ isotope ratio ($\delta^{2}H$) compared to OM derived from marine sources. The use of $\delta^{2}H$ in combination with more commonly employed stable isotopes with gradients across freshwater and marine habitats ($\delta^{13}C$) (Gearing, 1988) and trophic discrimination ($\delta^{15}N$) (Caut, Angulo, & Courchamp, 2009) provides a framework for tracing the contribution of riverine OM in glacial-marine food webs (Vander Zanden, Soto, Bowen, & Hobson, 2016).

Furthermore, riverine OM derived from glaciers is old (~2000–4,000 years BP ^{14}C-age) compared to non-glacial riverine OM, which is dominated by younger, plant-derived material (Hood et al., 2009; Singer et al., 2012). This ancient carbon derived from glacier ecosystems can be readily assimilated into terrestrial (Bardgett et al., 2007; Hågvar & Ohlson, 2013) and riverine food webs (Fellman et al., 2015), therefore we hypothesized that this ancient carbon subsidy may be an important resource to food webs at the glacial-marine interface.

We quantified the spatial extent and ecological impact of the flux of riverine OM into glacier-marine habitats. We used $\delta^{2}H$ water isoscape mapping to assess the scale of mixing and infiltration of glacier runoff into coastal waters and developed a multi-trophic three isotope Bayesian mixing model to estimate the contribution of riverine OM to glacial-marine food webs.

2 | MATERIALS AND METHODS

Our study area was focused within Prince William Sound, a coastal embayment ringed by a heavily glaciated mountain range in south-central Alaska (Figure 1). We also contrasted isotope compositions among species in glacially modified marine habitats with their counterparts from more oceanic habitats sampled in the western Aleutian Islands, which are isolated from the freshwater signal of the Alaska Coastal Current (Ladd, Hunt, Mordy, Salo, & Stabeno, 2005).

Because $\delta^{2}H$ values of consumer tissues reflect a blend of dietary and ambient water $\delta^{2}H$ conditions (Vander Zanden et al., 2016), we collected water samples to better understand the underlying hydrogen isoscape. Water samples were collected in Prince William Sound in 2012 and 2013 and in the Western Aleutians in 2013 (Figure 1). Freshwater samples for $\delta^{2}H$ and $\delta^{18}O$ analysis were collected from melt water runoff near recently grounded glaciers, and seawater samples were collected from 2 and 10 m depths in 4-L Niskin bottles. We also collected a water sample near the bottom, or to a maximum of 300 m depth (in 2013 only). These water samples were stored in tightly sealed 20 ml plastic vials with no headspace at room temperature until they could be processed in the lab.

Glacial runoff was collected in an acid-washed 4 L container from streams on the beach adjacent to recently grounded glaciers in Blackstone Bay (60° 39.805′N, 148° 39.587′W), Columbia Bay (61° 7.614′N, 147° 1.781′W), and Icy Bay (60° 10.626′N,148° 26.429′W). Seawater was collected in 4 L Niskin bottles using a Seabird Electronics SBE 19 plus v.2 conductivity-temperature-depth profiler equipped with an SBE55 auto-fire water sampler. Sample water was pre-filtered through a 150 μm mesh to remove zooplankton/detritus. Particulate OM (POM) was then filtered through a 47 mm glass fiber filter (0.7 μm) for stable isotopes or a pre-combusted (450°C for 4 hr) quartz filter (1.0 μm) for radiocarbon analysis (Fellman et al.,

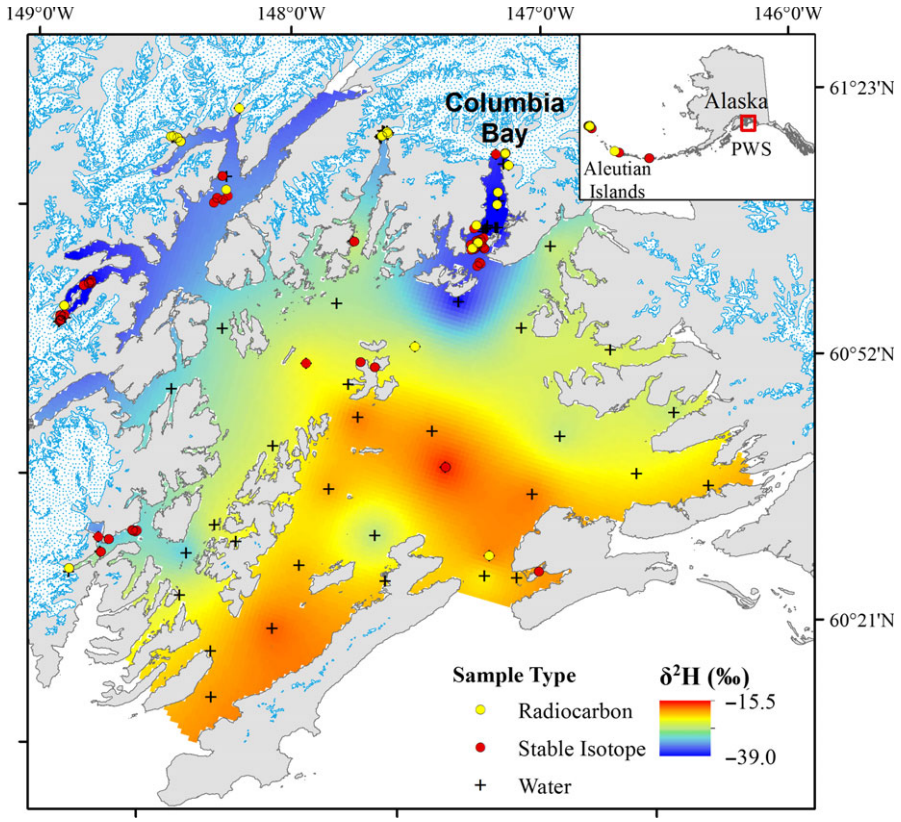

FIGURE 1 Map of the study area and Prince William Sound (PWS) hydrogen water isoscape (VSMOW-SLAP, krig predictions at 1 km^2 grid resolution) at 10 m water depth. Sample locations are indicated by sample type. All radiocarbon samples were also analyzed for stable isotopes. Stable isotope samples were accompanied by a water sample. The extent of glacier coverage (Pfeffer et al., 2014) is represented as blue stipple

2015). Due to high sediment load, the total volume of water filtered through each filter was generally less than 1.8 L. Approximately 1 L of filtrate was stored in acid-washed polycarbonate bottles for ^{14}C-dissolved organic carbon (DOC) analysis, and 250 ml of filtrate was stabilized with mercuric chloride and stored in a pre-combusted amber glass bottle (450°C for 4 hr) with no headspace for dissolved inorganic carbon (DIC) analysis (Caraco, Bauer, Cole, Petsch, & Raymond, 2010). The POM filters and DOC samples were frozen in the field, and DIC samples were stored at room temperature until they could be processed in the laboratory. Water samples were also frozen in acid-washed 60 ml HDPE bottles for analysis of inorganic nutrients (nitrate, NO_3; nitrite, NO_2; phosphate, PO_4; silicic acid, $SiOH_4$; and ammonium, NH_4).

Representative biota from coastal food web components were sampled in marine waters within five tidewater glacier fjords in Prince William Sound (Figure 1). We also opportunistically collected biota samples at oceanic Aleutian sites in coordination with a separate seabird diet study (Schoen et al., 2014). Bulk plankton samples were collected with a 150 μm mesh ring net on a 50 m vertical haul and the net contents were placed in filtered water for 3 hr to evacuate any gut contents. After ~1 ml of bulk plankton was placed in a vial, 20–40 large copepods (if they occurred within the sample) were individually removed from the remaining bulk plankton sample and placed in a vial and frozen with ~1 ml of seawater. Copepods were identified to species in the lab; *Calanus marshallae* and *Neocalanus flemingeri* were the dominant large copepod species, while *Pseudocalanus* spp. and *Acartia longiremis* were the dominant small copepod in preserved samples. Krill (*Euphausia pacifica*, and *Thysanoessa* spp. including a mix of *T. inermis*, *T. longipes*, *T. raschii*, *T. spinifera*), mysids *Neomysis rayii*, amphipods *Themisto libellula*, young of the year (YOY) fish (capelin, *Mallotus villosus*; Pacific herring, *Clupea pallasii*; and walleye pollock, *Gadus chalcogrammus*), and age 1+ fish (capelin; herring; pollock; eulachon, *Thaleichthys pacificus*) were collected with a modified herring trawl towed at depths greater than 20 m. Pacific sand lance *Ammodytes personatus* were collected with a beach seine. Whole crustaceans were placed in a vial and frozen in the field. Fish dorsal muscle tissue was excised and placed in a vial and frozen in the field, or sometimes whole fish were frozen and muscle tissue was excised in the lab. Mussels *Mytilus trossulus* were collected in the intertidal zone near glacier river outflows. Benthic organisms (marine sponge *Suberites* sp.; marine snails *Fusitriton oregonensis* and *Colus halli*; and shrimp *Pandalus hypsinotus*) collected in a trawl near tidewater glaciers were frozen whole until they could be processed in the lab. The seabirds Kittlitz's murrelets and marbled murrelets were captured using the night lighting technique (Whitworth, Takekawa, Carter, & McIver, 1997). Blood was drawn from

the tarsal vein of murrelets and frozen in glass vial in the field. The seabird black-legged kittiwakes *Rissa tridactyla* were collected with a shot gun, and liver samples were frozen individually in glass vials. Replicate samples of a subset of biota from each taxon were placed in precombusted glass vials and frozen in the field for $\Delta^{14}C$ analysis.

POM filters were oven dried at 50°C for 48 hr, and acidified with concentrated sulfurous acid to remove inorganic carbon. $\delta^{13}C$ and $\delta^{15}N$ analyses of POM were performed at UC Davis Stable Isotope Facility and within-run replicate of the laboratory standards had standard deviations of <0.1‰ for $\delta^{13}C$ and <0.2‰ for $\delta^{15}N$.

Plankton (>150 μm) and other biota samples ($\delta^{2}H$, $\delta^{13}C$, and $\delta^{15}N$), as well as water samples ($\delta^{2}H$ and $\delta^{18}O$) were processed at the Environment Canada lab, Saskatchewan. Samples were thawed, rinsed in distilled water, oven dried (plankton) or freeze dried (all other organisms) for 48 hr, powdered and treated with 2:1 chloroform methanol solution to account for variable lipid content across species and trophic levels through lipid removal. Lipids are also depleted in ^{13}C and ^{2}H and so need to be removed to avoid complications with the use of mixing models (Soto, Wassenaar, & Hobson, 2013). Crustaceans were soaked in 0.1 N HCl to remove carbonates without rinsing. Stable carbon and stable nitrogen isotope assays were performed on 1 mg samples of homogenized materials by combustion at 850°C in a Robo-Prep elemental analyzer. CO_2 and N_2 gases were analyzed with an interfaced 20:20 continuous flow isotope ratio mass spectrometer (Europa Scientific, Inc.) with every five unknowns separated by two (egg albumen) laboratory standards. Based on within-run replicate measurements of the laboratory standard, we estimated measurement error as ±0.1‰ for $\delta^{13}C$ and ±0.2‰ for $\delta^{15}N$.

Water isotopes ($\delta^{2}H$ and $\delta^{18}O$) were determined using off-axis integrated-cavity output laser spectroscopy (Model DLT-100; Los Gatos Research Inc.) following Lis, Wassenaar, and Hendry (2008). All samples were normalized to internal laboratory water standards previously calibrated relative to Vienna Standard Mean Ocean Water VSMOW (0‰) and Vienna Standard Light Antarctic Precipitation (VSLAP, $\delta^{2}H$ −428‰ and $\delta^{18}O$ −55.5‰). Stable-hydrogen isotope analyses of organic materials were conducted using the comparative equilibration method (Wassenaar & Hobson, 2003) through the use of calibrated keratin hydrogen-isotope reference materials (CBS: −197‰, SPK: −121.6‰, KHS: −54.1‰). The $\delta^{2}H$ isotope measurements were performed on H_2 derived from high-temperature (1,350°C) flash pyrolysis of 350 ± 10 μg tissue subsamples using continuous-flow isotope-ratio mass spectrometry (Isoprime, Manchester UK). Within-run (n = 5) measurement of the three keratin laboratory reference materials (CFS, CHS, BWB) indicated measurement error <2‰.

Natural abundance $\Delta^{14}C$ was analyzed for a subset of samples from each focal food web component at Woods Hole Oceanographic Institute by accelerator mass spectrometry following Raymond and Bauer (2001). Samples for analyses of $\Delta^{14}C$ in DOC, DIC, POM, and biota were acidified with concentrated sulfurous acid to remove carbonates, combusted at 900°C in double sealed quartz tubes, and the evolved CO_2 was purified and quantified on the vacuum extraction line (Druffel, Williams, Bauer, & Ertel, 1992). Isotope abundance is expressed in δ notation as the deviation from standards in parts per mil (‰) according to the following equation:

$$\delta X = \left[\left(\frac{R_{\text{sample}}}{R_{\text{standard}}}\right) - 1\right] \times 1{,}000 \quad (1)$$

where X is ^{13}C, ^{15}N, or ^{2}H, and R is the corresponding ratio $^{13}C/^{12}C$, $^{15}N/^{14}N$, or $^{2}H/^{1}H$. R_{standard} is based on Vienna PeeDee Belemnite (VPDB) for $\delta^{13}C$, atmospheric N_2 for $\delta^{15}N$, and VSMOW-SLAP for $\delta^{2}H$.

Reported $\Delta^{14}C$ values were corrected for fractionation using the $\delta^{13}C$ values of the samples. Most samples had paired measures, however, $\delta^{13}C$ samples were lost in a small number of cases. We substituted the nearest within-fjord $\delta^{13}C$ value for two POM samples with missing $\delta^{13}C$ values, and substituted the DIC $\delta^{13}C$ value of a sample with the most similar $\delta^{2}H$ water value for three missing DIC $\delta^{13}C$ measures. Because there was relatively little change in coastal marine DIC $\delta^{13}C$ (−0.8‰ at 2 m depth, or 0.2‰ at 160 m depth) the difference in $\Delta^{14}C$ value when substituting one $\delta^{13}C$ value or the other was 2‰, and less than the range of expected error (5‰–10‰).

To identify geographic patterns in the underlying $\delta^{2}H$ isoscape, we used geostatistics to graphically represent the extent of mixing and infiltration of cold, fresh glacier runoff into the coastal waters. We interpolated $\delta^{2}H$ values between 10 m depth water sample locations using ordinary kriging (Cressie, 1988). The $\delta^{2}H$ values were linearly related to X and Y coordinates (OLS, $p < .001$), therefore we applied a first order trend and robust estimator when computing the sample variogram. We used an exponential covariance model and iteratively estimated the nugget, sill and range parameters first with weighted least squares (WLS) regression, and then with restricted maximum likelihood (REML) parameter estimation using the WLS parameters as initial values (Diggle & Ribeiro, 2007). These analyses were accomplished with the "geoR" package (Ribeiro & Diggle, 2015) in R v. 3.3.3 (R Core Team, 2017). Krig predictions were made at a 1 km grid resolution within Prince William Sound.

We developed a three-isotope Bayesian mixing model to estimate trophic position τ and basal source contributions φ_{jl} to the pelagic food web in Prince William Sound. Let i be an individual, let j be a species (or species group), let k be a taxon-specific tissue and let l be a source (offshore, coastal or freshwater). The trophic position τ for species j is

$$\tau_j = 2 + \frac{\delta^{15}N_j^{\text{obs}} - \delta^{15}N_{\text{base}}}{\Delta N_{jk}} \quad (2)$$

where $\delta^{15}N_j^{\text{obs}}$ is the $\delta^{15}N$ value of consumer tissues for species j, $\delta^{15}N_{\text{base}}$ is the $\delta^{15}N$ value of baseline consumers (i.e., copepods in this nearshore pelagic system), and is the per-trophic level discrimination factor for $\delta^{15}N$ by taxon-specific tissue for each species. The total trophic discrimination for ^{13}C and ^{15}N for species j, f_j^C and f_j^N, respectively, incorporate taxon-specific tissue discrimination, $\Delta^{13}C_{jk}$ and $\Delta^{15}N_{jk}$, (here Δ notation represents the change in δX) of trophic

levels below species j

$$f_j^{\mathrm{C}} = \Delta^{13}\mathrm{C}_{jk} \times (\tau_j - 1) \text{ and } f_j^{\mathrm{N}} = \Delta^{15}\mathrm{N}_{jk} \times (\tau_j - 1) \quad (3)$$

The expected $\delta^{13}C_j$ and $\delta^{15}N_j$ for species j is estimated to be a function of the $\delta^{13}C$ and $\delta^{15}N$ signatures of source l (s_l^{C} and s_l^{N}), the trophic discrimination for species j (f_j^{C} and f_j^{N}), and the proportion that species j feeds upon each source l (φ_{jl}). We assume source contributions sum to 1

$$\delta^{13}\mathrm{C}_j = \sum_{l=1}^{3} \varphi_{jl}\left(s_l^{\mathrm{C}} + f_j^{\mathrm{C}}\right) \text{ and } \delta^{15}\mathrm{N}_j = \sum_{l=1}^{3} \varphi_{jl}\left(s_l^{\mathrm{N}} + f_j^{\mathrm{N}}\right) \quad \text{where } \sum_j \varphi_{jl} = 1\ \forall \quad (4)$$

The standard deviations of $\delta^{13}C_j$ and $\delta^{15}N_j$ (σ_j^{C} and σ_j^{N}) are a function of the variance of proportions of l sources for species j, φ_{jl}^2, the standard deviation of each source ($\sigma_l^{s^{\mathrm{C}}}$ and $\sigma_l^{s^{\mathrm{N}}}$) and the standard deviation of total isotopic discrimination for species j ($\sigma_j^{f^{\mathrm{C}}}$ and $\sigma_j^{f^{\mathrm{N}}}$)

$$\sigma_j^{\mathrm{C}} = \sqrt{\sum_{l=1}^{3} \varphi_{jl}^2\left(\left(\sigma_l^{s^{\mathrm{C}}}\right)^2 + \left(\sigma_j^{f^{\mathrm{C}}}\right)^2\right)} \text{ and } \sigma_j^{\mathrm{N}} = \sqrt{\sum_{l=1}^{3} \varphi_{jl}^2\left(\left(\sigma_l^{s^{\mathrm{N}}}\right)^2 + \left(\sigma_j^{f^{\mathrm{N}}}\right)^2\right)} \quad (5)$$

The expectation and standard deviation of δ^2H differs from $\delta^{13}C$ and $\delta^{15}N$ because the δ^2H ratio in consumer tissues is influenced by δ^2H values of environmental water, $\delta^2H_j^w$ in addition to δ^2H values of dietary sources. There is a large photosynthetic discrimination (Δ^2H) between water and primary producers (Finlay, Doucett, & McNeely, 2010; Sessions, Burgoyne, Schimmelmann, & Hayes, 1999; Yang, Wilkinson, Cole, Macko, & Pace, 2014), but we assume no trophic discrimination at higher trophic levels (Solomon et al., 2009; Soto et al., 2013). For kittiwakes, we included an additional isotopic discrimination term, f_{BLKI}^H, to account for isotopic discrimination apparent in exploratory analyses (Fig. S1). This isotopic variability likely reflects tissue-specific discrimination or other unknown source of variability (see Ostrom, Wiley, Rossman, Stricker, & James, 2014), which is currently poorly known for ^2H in food webs but is consistently observed in other isotopes (Hobson, 1993; Mizutani, Kabaya, & Wada, 1991; Quillfeldt, Bugoni, McGill, Masello, & Furness, 2008). Seabird blood (sampled in murrelets only), did not show additional ^2H isotopic discrimination with respect to the rest of the food web (Fig. S1). Let ω_j be the proportion of δ^2H in consumer tissues due to water. The expected δ^2H_j is:

$$\delta^2\mathrm{H}_j = \begin{cases} (\omega_j \times \delta^2\mathrm{H}_j^{\mathrm{w}}) + (1-\omega_j)\sum_{k=1}^{3} \varphi_{jl}\left(s_l^{\mathrm{H}} + \Delta^2\mathrm{H}\right) & \text{if } j \neq \mathrm{BLKI} \\ f_{\mathrm{BLKI}}^{\mathrm{H}} + (\omega_{\mathrm{BLKI}} \times \delta^2\mathrm{H}_{\mathrm{BLKI}}^{\mathrm{w}}) + (1-\omega_{\mathrm{BLKI}})\sum_{l=1}^{3} \varphi_{jl}\left(s_l^{\mathrm{H}} + \Delta^2\mathrm{H}\right) & \text{if } j = \mathrm{BLKI} \end{cases} \quad \text{where } \sum_j \varphi_{jl} = 1\ \forall \quad (6)$$

The standard deviation σ_j^{H} is a function of variance of proportions of l sources for species j, φ_{jl}^2, the standard deviation of each source ($\sigma_l^{s^{\mathrm{H}}}$) and the standard deviation of photosynthetic discrimination ($\sigma^{\Delta^2\mathrm{H}}$) and the standard deviation of the proportion of δ^2H due to environmental water (σ_j^{ω}). For kittiwakes we include an additional error term for isotopic discrimination, $\sigma^{f_{\mathrm{BLKI}}^{\mathrm{H}}}$

$$\sigma_j^{\mathrm{H}} = \begin{cases} \sqrt{\sum_{l=1}^{3} \varphi_{jk}^2\left(\left(\sigma_l^{s^{\mathrm{H}}}\right)^2 + \left(\sigma^{\Delta^2\mathrm{H}}\right)^2 + \left(\sigma_j^{\omega}\right)^2\right)} & \text{if } j \neq \mathrm{BLKI} \\ \sqrt{\sum_{l=1}^{3} \varphi_{jl}^2\left(\left(\sigma_l^{s^{\mathrm{H}}}\right)^2 + \left(\sigma^{\Delta^2\mathrm{H}}\right)^2 + \left(\sigma_{\mathrm{BLKI}}^{\omega}\right)^2 + \left(\sigma^{f_{\mathrm{BLKI}}^{\mathrm{H}}}\right)^2\right)} & \text{if } j = \mathrm{BLKI} \end{cases} \quad (7)$$

For individual i of species j, $\delta^{13}C_{ij}^{\mathrm{obs}}$, $\delta^{15}N_{ij}^{\mathrm{obs}}$ and $\delta^2H_{ij}^{\mathrm{obs}}$ in consumer tissues are assumed to be normally distributed about the expected value of each isotope for species j, $\delta^{13}C_j$, $\delta^{15}N_j$, and δ^2H_j with standard deviation σ_j^{C}, σ_j^{N} and σ_j^{H}

$$\begin{aligned} \delta^{13}\mathrm{C}_{ij}^{\mathrm{obs}} &= \delta^{13}\mathrm{C}_j + \varepsilon_i^{\mathrm{C}} \quad \text{where } \varepsilon_i^{\mathrm{C}} \sim \mathrm{N}\left(0,\ \left(\sigma_j^{\mathrm{C}}\right)^2\right) \\ \delta^{15}\mathrm{N}_{ij}^{\mathrm{obs}} &= \delta^{15}\mathrm{N}_j + \varepsilon_i^{\mathrm{N}} \quad \text{where } \varepsilon_i^{\mathrm{N}} \sim \mathrm{N}\left(0, \left(\sigma_j^{\mathrm{N}}\right)^2\right) \\ \delta^2\mathrm{H}_{ij}^{\mathrm{obs}} &= \delta^2\mathrm{H}_j + \varepsilon_i^{\mathrm{H}} \quad \text{where } \varepsilon_i^{\mathrm{H}} \sim \mathrm{N}\left(0, \left(\sigma_j^{\mathrm{H}}\right)^2\right) \end{aligned} \quad (8)$$

The likelihood for this model for $i = 1$ to m individuals, and $j = 1$ to n species groups is:

$$\begin{aligned} L(x \mid \varphi, y, \sigma) = &\prod_{i=1}^{m}\prod_{j=1}^{n}\left(\frac{1}{\sigma_j^{\mathrm{C}}\sqrt{2\pi}}\exp\left[\frac{1}{2\left(\sigma_j^{\mathrm{C}}\right)^2}\left(\delta^{13}\mathrm{C}_{ij}^{\mathrm{obs}} - \delta^{13}\mathrm{C}_j\right)^2\right]\right) \\ &\times \prod_{i=1}^{m}\prod_{j=1}^{n}\left(\frac{1}{\sigma_j^{\mathrm{N}}\sqrt{2\pi}}\exp\left[\frac{1}{2\left(\sigma_j^{\mathrm{N}}\right)^2}\left(\delta^{15}\mathrm{N}_{ij}^{\mathrm{obs}} - \delta^{15}\mathrm{N}_j\right)^2\right]\right) \\ &\times \prod_{i=1}^{m}\prod_{j=1}^{n}\left(\frac{1}{\sigma_j^{\mathrm{H}}\sqrt{2\pi}}\exp\left[\frac{1}{2\left(\sigma_j^{\mathrm{H}}\right)^2}\left(\delta^2\mathrm{H}_{ij}^{\mathrm{obs}} - \delta^2\mathrm{H}_j\right)^2\right]\right) \end{aligned} \quad (9)$$

We used prior information (Table 1), including published and sample data to estimate posterior distributions of model parameters. To calculate trophic position, we assumed a normal distribution of $\delta^{15}N$ in secondary consumers and baseline consumers (i.e., Calanoid copepods) with a mean and *SD* equal to that of each sampled species group (Table 2). We assumed offshore sources were normally distributed with published mean ± *SD* of $\delta^{13}C = -24.2 \pm 1.3‰$ and $\delta^{15}N = 3.0 \pm 0.8‰$ in OM measured in the in the Gulf of Alaska (n = 4, Wu, Calvert, Wong, & Whitney, 1999; n = 7, Walinsky et al., 2009; see Supporting information). These data are in line with data for primary consumers (copepods, mean ± *SD* $\delta^{13}C = -23.3 \pm 2.0‰$; $\delta^{15}N = 7.3 \pm 2.5‰$, n = 1,590; Kline, 2009).

Coastal source priors for $\delta^{13}C$ and $\delta^{15}N$ were normally distributed with mean ± *SD* $\delta^{13}C = -20.6 \pm 1.6‰$; $\delta^{15}N = 3.9 \pm 1.1‰$, based on the mean of published values of OM from glacial inlets in the region (n = 5, Walinsky et al., 2009) and >150 μm plankton samples from coastal marine waters that had $\delta^{15}N$ values consistent with primary producers (n = 3, this study, Table S1). Glacial riverine OM

TABLE 1 Prior distributions of multi-trophic Bayesian isotope mixing model parameters. Numbers in bold represent standard deviations (*SD*) that were increased relative to actual SDs due to low sample size (see supplemental information for source data)

Parameter type	Parameter name	*n*	Mean	*SD*	Min	Max	Prior distribution
Isotope ratio	δ^{15}N baseline consumer (‰)	4	7.0	1.4			N(mean, *SD*)
Isotope ratio	δ^{15}N of each species group (‰)		Mean δ^{15}N by species	*SD* δ^{15}N by species			N(mean, *SD*)
Source	Coastal OM δ^{13}C (‰)[a]	8	−20.6	1.6			N(mean, *SD*)
Source	Coastal OM δ^{15}N (‰)[a]	8	3.9	1.1			N(mean, *SD*)
Source	Coastal Water δ^{2}H (‰)	10	−17.4	9.8			N(mean, *SD*)
Source	Ocean OM δ^{13}C (‰)[b]	18	−24.2	1.3			N(mean, *SD*)
Source	Ocean OM δ^{15}N (‰)[b]	19	3.0	0.8			N(mean, *SD*)
Source	Ocean Water δ^{2}H (‰)	3	−7.3	**10.0**			N(mean, *SD*)
Source	Riverine OM δ^{13}C (‰)[a]	9	−25.0	1.3			N(mean, *SD*)
Source	Riverine OM δ^{15}N (‰)	3	4.4	3.9			N(mean, *SD*)
Source	Riverine Water δ^{2}H (‰)	4	−113.0	10.9			N(mean, *SD*)
Discrimination	ΔC (all tissues, ‰)[c]		0.4	1.3			N(mean, *SD*)
Discrimination	ΔN (seabird liver, ‰)[d]		3.0	0.9			N(mean, *SD*)
Discrimination	ΔN (seabird blood, ‰)[d]		2.2	0.7			N(mean, *SD*)
Discrimination	ΔN (fish muscle, ‰)[d]		3.2	1.9			N(mean, *SD*)
Discrimination	ΔN (fish whole, ‰)[d]		2.2	1.1			N(mean, *SD*)
Discrimination	ΔN (invertebrate whole, ‰)[d]		2.3	0.9			N(mean, *SD*)
Discrimination	ΔH (water-phytoplankton, ‰)[e]		−163.7	27.0			N(mean, *SD*)
Discrimination	Kittiwake liver discrimination (‰)				30	150	U(min, max)
Proportion ^{2}H due to water	ω (seabird, proportion) [f]		$1-(1-0.23)^{\tau-1}$	**0.05**		0.7	N(mean, *SD*)
Proportion ^{2}H due to water	ω (fish, proportion) [g]		0.33	0.1		0.7	N(mean, *SD*)
Proportion ^{2}H due to water	ω (zooplankton, proportion)		0.23	0.03		0.7	N(mean, *SD*)
Sigma	*SD* sources, discrimination				0	10,000	U(min, max)

OM, organic matter, τ, trophic position; N, normal distribution; U, uniform prior.
[a]Walinsky et al. (2009), this study, Table S1; [b]Walinsky et al. (2009), Wu et al. (1999); [c]Post (2002); [d]Caut et al. (2009); [e]Finlay et al. (2010), Yang et al. (2014), Solomon et al. (2011); [f]Solomon et al. (2009), Soto et al. (2013), Wilkinson et al. (2015); [g]Soto et al. (2013), Wilkinson et al. (2015); [h]Solomon et al. (2009), Wilkinson et al. (2015).

source δ^{13}C was assumed to be normally distributed with mean ± *SD* δ^{13}C = −25.0 ± 1.3‰, based on the mean of published (*n* = 6, Walinsky et al., 2009) and sampled (*n* = 3, Table S1) values of POM from glacier rivers. These freshwater source values aligned with published world riverine OM δ^{13}C = −26.4 ± 1.5‰ (Gearing, 1988). Glacial riverine OM source prior for δ^{15}N was assumed to be normally distributed with mean ± *SD* = 4.4 ± 3.9‰, based on riverine OM samples collected in this study (*n* = 3, Table S1). Although the sample size was low due to the difficulty in attaining these samples, the relatively large *SD* specified for this prior represents the expected variability in this parameter.

Basal sources of δ^{2}H were the measured δ^{2}H abundance of water in offshore marine, coastal marine and glacial freshwater. We assumed δ^{2}H sources were normally distributed with a mean ± *SD* of water samples (Table 1, see also Supporting information). Offshore source water was −7.3 ± 1.3‰ (*n* = 3), coastal source water (i.e., >50 m depth and salinity >28 to exclude surface waters with freshwater influence) was −17.4 ± 9.8‰ (*n* = 10), and glacial stream water above the tideline was −113.0 ± 10.9‰ (*n* = 4). Due to low variability in offshore water source samples, we increased the prior *SD* for this parameter to 10‰ to facilitate MCMC sampling over a range similar to other sources.

We assumed trophic discrimination factors of δ^{13}C and δ^{15}N varied by taxa and tissue (i.e., bird liver, bird blood, whole fish, fish muscle, macro- and microzooplankton whole invertebrates, Caut et al., 2009). We assumed per-trophic level discrimination factors were normally distributed with mean ± *SD* of 0.4 ± 1.3‰ for $\Delta^{13}C_k$ (Post, 2002; Vander Zanden & Rasmussen, 2001) and between 2.2‰ and 3.2‰ (*SD* range 0.7–1.9) for $\Delta^{15}N_k$ (Table 1) based on data from similar taxa-tissue types (Caut et al., 2009). Lower and upper bounds of trophic position were set between 1.8 and 5.5. Due to the difficulty of isolating δ^{2}H abundance in the autotrophic component of riverine OM we used indirect methods to estimate photosynthetic discrimination between δ^{2}H in water and that of primary consumers following Solomon et al. (2011). Photosynthetic discrimination (Δ^{2}H) between phytoplankton and water was assumed to be normally distributed with a mean ± *SD* = −163.7 ± 27.0‰, which corresponds to values reported from freshwater and marine systems (Doucett, Marks, Blinn, Caron, & Hungate, 2007; Finlay et al., 2010; Sessions et al., 1999; Solomon et al., 2011; Yang et al., 2014). Our lipid-free estimates of

TABLE 2 Mean (*SD*) stable isotope composition (‰) and fish size (mean *SD*) of pelagic food web components sampled in July 2012 and 2013 in Prince William Sound and Aleutian Islands, Alaska

	Glacial-marine habitat				Oceanic habitat			
Species	*n*	δ^2H	δ^{15}N	δ^{13}C	*n*	δ^2H	δ^{15}N	δ^{13}C
Black-legged kittiwake (seabird liver)	28	−37.1 (11.2)	15.9 (0.5)	−18.3 (0.5)				
Kittlitz's murrelet (seabird blood)	21	−106.6 (6.2)	14.8 (0.4)	−19.0 (0.8)	1	−91.3	10.4	−22.7
Marbled murrelet (seabird blood)	18	−91.6 (6.5)*	15.2 (0.4)*	−18.6 (0.4)*	4	−75.5 (3.1)*	10.9 (0.9)*	−22.7 (0.2)*
Capelin (fish muscle, 96 ± 16 mm)	43	−128.5 (13.1)	13.2 (0.4)	−19.0 (0.3)				
Eulachon (fish muscle, 107 ± 34 mm)	22	−158.6 (29.4)	14.8 (0.6)	−19.4 (1.4)				
Pacific herring (fish muscle, 129 ± 33 mm)	29	−118.2 (11.5)	13.5 (0.5)	−19.1 (0.4)				
Walleye pollock (fish muscle, 275 ± 78 mm)	40	−133.7 (11.9)	13.5 (0.8	−18.6 (0.6)				
Pacific sand lance (fish muscle, 106 ± 38 mm)	26	−126.4 (8.1)	12.3 (0.4)*	−19.4 (0.6)*	7	−127.1 (3.1)	9.0 (0.1)*	−22.6 (0.3)*
YOY capelin (fish muscle, 32 ± 3 mm)	12	−133.6 (4.2)	11.6 (0.3)	−19.9 (0.8)				
YOY Pacific herring (fish muscle, 35 ± 5 mm)	40	−141.8 (11.0)	11.5 (0.5)	−20.3 (0.7)				
YOY walleye pollock (fish muscle, 49 ± 10 mm)	42	−148.2 (12.6)*	11.7 (0.6)*	−19.5 (0.6)	6	−125.85 (6.89)*	10.2 (0.5)*	−19.9 (1.2)
Euphausia pacifica (krill, whole)	37	−135.8 (14.3)	11.0 (1.2)	−18.8 (0.5)				
Neomysis rayii (mysid, whole)	16	−128.5 (5.5)	12.4 (0.5	−18.4 (0.2)				
Themisto libellula (amphipod, whole)	15	−136.7 (4.6)	11.2 (0.5)	−18.0 (0.2)				
Thysanoessa spp. (krill, whole)	30	−157.1 (10.7)*	9.9 (0.6)*	−18.4 (0.8)*	6	−145.6 (2.4)*	7.9 (1.0)*	−20.8 (1.1)*
Bulk zooplankton (>150 μm)	6	−164.4 (8.1)	7.4 (1.2)	−19.8 (0.5)	1	−150.3	6.0	−22.2
Calanoid copepod (>150 μm)	4	−138.3 (8.5)	7.0 (1.4)	−20.2 (0.4)	1	−129.3	6.6	−22.1
Mytilus trossulus (mussel, muscle)	19	−152.8 (15.3)*	7.6 (0.8)	−19.1 (0.5)*	4	−95.2 (5.2)*	8.1 (0.5)	−15.9 (0.2)*
Suberites sp. (sponge, whole)	1	−86.1	7.2	−18.2				
Fusitriton oregonensis (snail, foot)	2	−87.1 (1.2)	12.0 (0.8)	−17.5 (0.1)				
Colus halli (snail, foot)	1	−66.5	13.9	−16.2				
Pandalus hypsinotus (shrimp, whole)	1	−105.8	11.8	−15.7				

Due to size and life-history differences, young of the year (YOY) fish are separated from age 1+ year classes. Lipids were extracted from all biota samples prior to analysis. Asterisks (*) indicates, for taxa with more than one sample at both sites, >95% probability that mean difference in corresponding isotope values between sites was different from 0.

Δ^2H from 3 coastal phytoplankton (>150 μm) samples had a mean ± *SD* = −140.49 ± 27.2‰ (Table S1). Laboratory studies suggest the proportion of δ^2H in consumer tissues due to environmental water (ω) ranges from 0.24 to 0.69 across trophic levels in aquatic systems (Solomon et al., 2009), thus we set the upper limit for ω at 0.7. Prior distributions for ω by species group were assumed to be normally distributed with mean ± *SD* equal to those provided from published studies, i.e., 0.23 ± 0.03 for zooplankton (Wilkinson, Cole, & Pace, 2015) and 0.33 ± 0.10 for fish (Soto, Wassenaar, Hobson, Catalan, & Trudel, 2011). Due to their higher trophic levels (τ), we applied the trophic compounding equation (Solomon et al., 2009; Vander Zanden et al., 2016) to estimate ω for seabirds, such that $\omega_{seabird} = 1 - (1 - 0.23)^{\tau - 1}$. The prior distribution was assumed to be a normal distribution with mean $\omega_{seabird}$, and we increased the *SD* from the reported *SD* of 0.03 (Wilkinson et al., 2015) to 0.05 to reflect greater uncertainty in the highest trophic levels. We applied an uninformative uniform prior for f^H_{BLKI} between 30‰ and 150‰ based on exploratory data analysis (Fig. S1). Standard deviations for source and discrimination were given a uniform prior from 0 to 10,000. Source proportions φ_{jk} had no priors set, but were defined as the unit simplex (Erhardt, Wolf, Ben-David, & Bedrick, 2014) such that k sources were non-negative and summed to 1.

Markov chain Monte Carlo (MCMC) was run for 10^6 iterations, with a burn-in of 10^5 iterations and a thinning rate of 900, which resulted in 1,000 samples of the posterior distribution. We used Stan (Stan Development Team 2016) implemented in R v. 3.3.3 (R Core Team, 2017). We chose this software over others because it compiles into C++ programming language, and also handles complex models more efficiently by implementing a gradient-based No-U-Turn sampling system (Hoffman & Gelman, 2014). Visual inspection of trace plots for model parameters indicated adequate convergence of model parameters, and posterior predictive distributions were evaluated to assess model fit (Figs S2–S5). Source and biota isotope data, as well as model code are provided in the Supporting information. In addition, all the data from this study are available at https://alaska.usgs.gov/products/data.php?dataid=139.

3 | RESULTS

The water hydrogen isoscape identified the lower δ^2H freshwater signal around the periphery of the embayment due to cold, fresh glacial runoff in the more heavily glaciated areas of the fjords (Figure 1). Cold freshwater runoff from Columbia Glacier, the largest

tidewater glacier in Alaska, can be identified in the hydrogen isoscape by lower water δ^2H values up to 45 km away from the glacier face. The warmer and higher salinity Gulf of Alaska coastal waters are distinct in surface waters of the southern and central regions of the embayment, consistent with the dominant circulation of Alaska Coastal Current waters through the region (Niebauer, Royer, & Weingartner, 1994).

Glacier-dominated riverine, coastal and offshore sources were distinguished by their δ^{13}C and δ^2H values (Table S1). Coastal OM δ^{13}C values were distinctly higher than other sources (range: −22.4‰ to −17.7‰), and although POM δ^{13}C values overlapped in riverine (range: −26.3‰ to −22.5‰) and offshore sources (range: −27.3‰ to −22.2‰), we identified a strong gradient in δ^2H values between glacier-dominated riverine water (range: −128.6‰ to −104.4‰) and marine water sources (range coastal: −43.5‰ to −7.5‰, range offshore: −8.12‰ to −5.7‰). Riverine OM (range: 2.1‰–8.9‰), coastal (range: 2.5‰–5.5‰) and offshore (range: 1.6‰–4.4‰) OM sources had overlapping δ^{15}N values, but riverine values were more variable.

The POM in glacial runoff and near surface coastal waters was depleted in ^{14}C (−780‰ to −176‰, 12,100–1,500 years BP ^{14}C-age, Table 3). Likewise, dissolved organic carbon (DOC, −294 and −298‰; 2,740 and 2,780 years BP ^{14}C-age, respectively) in glacial runoff and near surface coastal waters and dissolved inorganic carbon (DIC) in glacial runoff (−272‰, 2,770 years BP ^{14}C-age) were also depleted in ^{14}C. In contrast, DIC from coastal waters were enriched in ^{14}C (−22‰ to 70‰, 515 years BP to modern). Phytoplankton (−50‰, 440 years BP ^{14}C-age) and biota (−60‰ to 8‰, 530 years BP to modern ^{14}C-age) were also enriched in ^{14}C relative to riverine OM. The fraction of modern carbon in DOC and POM was 0.71 (*SD* 0), and 0.55 (*SD* 0.2), respectively, but in phytoplankton, DIC and biota it ranged from 0.92 to 0.99. Furthermore, the fraction of modern carbon of biota in glacial-marine and oceanic habitats overlapped nearly completely (Table 3).

Riverine OM contributions to glacial-marine food webs varied by species as mean point estimates of posterior distributions ranged from 12% to 44% (Figure 2). The isotopic composition of several species of plankton-feeding fish (e.g., eulachon, herring, pollock, and sand lance, Iverson, Frost, & Lang, 2002), and the plankton and fish-feeding (Hatch, Robertson, & Baird, 2009) seabird black-legged kittiwakes reflected plasticity in feeding behavior and a relatively high level of uncertainty in estimates of source contributions (Figure 2; Table S2). In some taxa, however, source contribution estimates for relatively similar species showed marked differences. For example, despite their similar size, feeding habits and co-occurrence in Gulf of Alaska coastal waters, the glacier-nesting Kittlitz's murrelet rely on riverine OM sources to a greater extent than the congeneric marbled murrelet (mean ± *SD* = 41 ± 14% vs. 28 ± 13%, respectively).

Likewise, two krill groups separated at the genus level appear to have different feeding histories; *Euphausia* tissues reflected greater use of offshore and coastal resources (mean ± *SD* = 59 ± 12% and 25 ± 10%, respectively, Table S2) and *Thysanoessa* tissues reflected

TABLE 3 Summary of radiocarbon data, including the mean (*SD*) fraction modern carbon, Δ^{14}C (‰) and radiocarbon age by sample type at a glacially influenced coastal site (Prince William Sound) and an oceanic (Aleutian Islands) site in Alaska

	Glacial-Marine habitat				Oceanic habitat			
	n	Fraction Modern	Δ^{14}C	^{14}C Age	*n*	Fraction Modern	Δ^{14}C	^{14}C Age
DOC	2	0.71 (0)	−296 (1)	2,760 (28)				
POM (<150 μm)	8	0.55 (0.20)	−455 (196)	5,360 (3,448)				
Phytoplankton	1	0.95	−50	440				
DIC	6	0.92 (0.11)	−38 (120)	720 (1,022)[a]				
Mussel	1	0.94	−60	530	1	0.94	−53	525
Sponge	1	0.98	−10	130				
Snail	3	0.99 (0)	0 (3)	68 (33)				
Shrimp	1	0.99	3	65				
Copepod	1	0.97	−33	285	1	0.96	−44	345
Krill	5	0.98 (0.02)	−15 (17)	170 (128)[a]	1	0.92	−79	650
Capelin	3	0.98 (0.02)	−18 (16)	187 (127)				
Eulachon	1	0.97	−27	285				
Pacific herring	1	0.97	−20	220				
Walleye pollock	1	0.95	−41	370				
Kittlitz's murrelet	3	0.99 (0)	−9 (6)	95 (33)	1	0.98	−25	180
Black-legged kittiwake	1	0.98	−12	145				

DOC, dissolved organic carbon; POM, particulate organic matter; DIC, dissolved inorganic carbon.
[a]Modern samples were averaged as zero age.

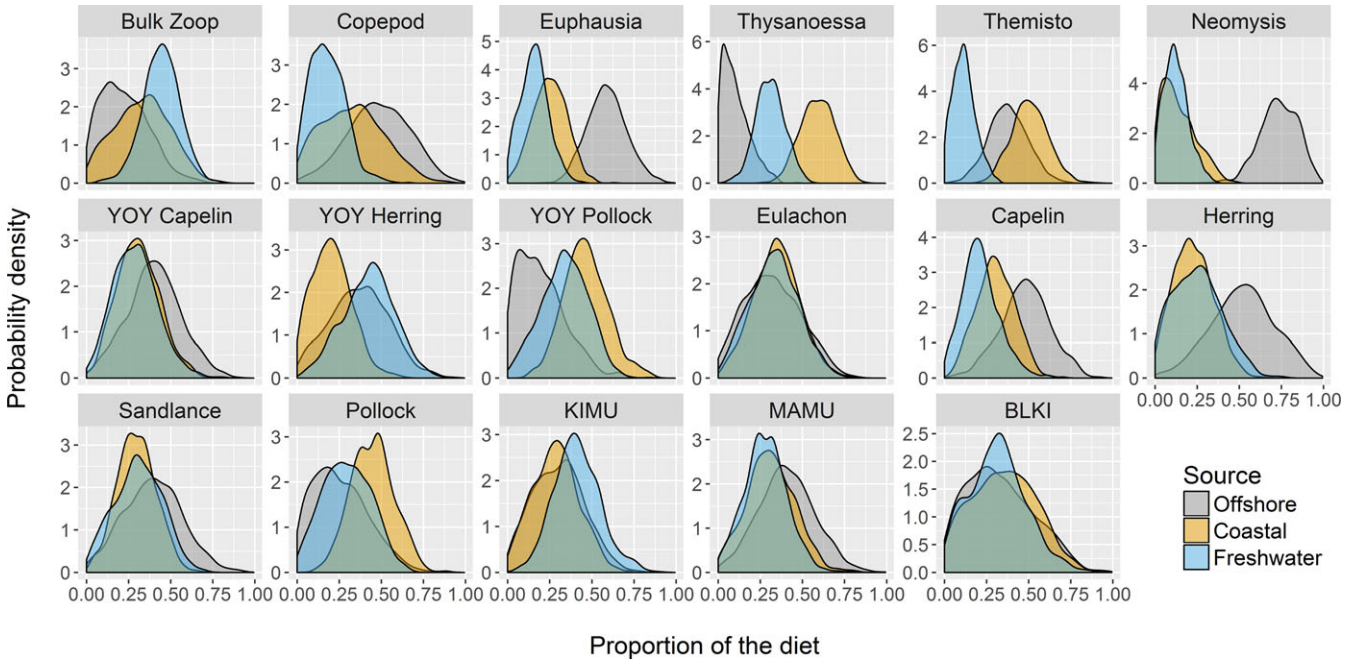

FIGURE 2 Posterior density distributions of source organic matter contributions to species in a coastal marine food web with tidewater glacier influence. YOY, young of the year; KIMU, Kittlitz's murrelet; MAMU, marbled murrelet; BLKI, black-legged kittiwake

greater use of coastal and riverine OM resources (mean ± *SD* = 59 ± 10% and 31 ± 9%, respectively). The relatively lower contribution of riverine OM sources to other macrozooplankton species, including the amphipod *Themisto* (mean ± *SD* = 12 ± 7%), mysid *Neomysis* (mean ± *SD* = 12 ± 7%), and krill *Euphausia* (mean ± *SD* = 16 ± 8%) suggest lower residence time in this system than *Thysanoessa*.

Despite potential differences in baseline isotopic compositions among large ecoregions, we pooled samples across several oceanic sampling sites (Figure 1) based on previous work that showed relative stability in isoscapes of primary consumers from the central to western Aleutians (Schell, Barnett, & Vinette, 1998). The $\delta^{13}C$ and $\delta^{15}N$ values of most biota sampled in glacial-marine habitats were distinct from those in oceanic habitats (Table 2). Bayesian estimation of the difference in means analysis (BEST, Kruschke, 2013) indicated intertidal mussels, representative of primary consumers, from glacial-marine habitats were depleted in both ^{13}C and ^{2}H compared to oceanic habitats (mean difference = −3.2‰ and −57.5‰, respectively), possibly reflecting greater availability of ^{13}C-enriched kelp-derived carbon (Bustamante & Branch, 1996), and ^{2}H-enriched seawater in the oceanic compared to the glacial-marine habitat. Credible intervals of $\delta^{15}N$ values of mussels at both sites overlapped, indicating primary consumer $\delta^{15}N$ values were not different between glacial and oceanic habitats. For two species of fish, credible intervals of young-of-the-year walleye pollock $\delta^{13}C$ values and sand lance $\delta^{2}H$ values overlapped between the two habitats. Otherwise, the pelagic food web in glacial habitats was ^{13}C-enriched and ^{2}H-depleted compared to oceanic habitats (Table 2). While differences in $\delta^{13}C$ in the food web across different oceanographic regions may be expected (Dunton, Saupe, Golikov, Schell, & Schonberg, 1989; Schell et al., 1998), similarity of mean $\delta^{15}N$ values among primary consumers (mussels, bulk zooplankton and copepods) suggest a common $\delta^{15}N$ baseline between the glacial-marine and oceanic habitats we sampled. We found that secondary and tertiary consumers (krill, fish and seabirds) from glacial-marine habitats had higher $\delta^{15}N$ values compared to oceanic habitats (Table 2). The patterns we observed, similarly documented in humpback whales isotope compositions throughout the N. Pacific (Witteveen, 2011), were mediated by omnivory at the krill level (see also Sprules & Bowerman, 1988). A divergence in food web structure may be related to differences in productivity between the large marine ecosystems we sampled (Yodzis, 1984), however, a full analysis is beyond the scope of this paper.

4 | DISCUSSION

We used multiple isotopic tracers to investigate the degree of biogeochemical connectivity between glacial watersheds and coastal ecosystems. Our work demonstrates the contemporary use of riverine OM by coastal food webs in a system that is undergoing globally significant change. In contrast to findings from freshwater and other aquatic ecosystems (Fellman et al., 2015; Guillemette, Bianchi, & Spencer, 2017), our findings suggest that the glacier-derived ancient carbon component of the riverine OM pool is not readily incorporated into marine food webs in glacier fjords despite the high lability of the bulk pool of glacier-derived OM (Hood et al., 2009). These findings from glacierized systems in the Gulf of Alaska concur with previous work using isotopic tracers in the Arctic, whereby aged riverine-derived peat was available and assimilated within the freshwater food web but not utilized by higher trophic organisms in the

coastal marine system (Schell, 1983). Given that stable isotope data suggest substantial contribution of terrigenous carbon to some species, we conclude the allochthonous subsidies to glacial-marine food webs are primarily composed of young riverine OM sources released from glacier ecosystems and their surrounding watersheds. This may arise because the relatively low OM content in glacier runoff (Fellman et al., 2010), which is just one component of the freshwater discharge into the system (Hill, Bruhis, Calos, Arendt, & Beamer, 2015).

An important control on the variability in the assimilation of riverine OM subsidies among species is differential habitat use, or the amount of time spent foraging by a given species near glacier outflows during peak melt season. For example, Kittlitz's murrelets tend to be associated with glacier ice (Arimitsu et al., 2012) and feed at a slightly lower trophic level than marbled murrelets (Hobson, Piatt, & Pitocchelli, 1994; Table S2). During the summer breeding season, Kittlitz's murrelets regularly feed on forage fish and krill within the turbid glacier plume because they are uniquely adapted to foraging conditions in close proximity to their nests on or near tidewater glaciers (Arimitsu et al., 2012). Marbled murrelets, on the other hand, obtain a lower proportion of their food resources from riverine OM sources by feeding throughout Gulf of Alaska coastal waters (Arimitsu, Piatt, Romano, Madison, & Conaway, 2010), although they are known to forage in freshwater lakes in some parts of their range (Hobson, 1990). Similarly, patterns of coastal and offshore resource use in krill are consistent with the relative oceanic (*Euphausia pacifica*) vs. neritic (*Thysanoessa* spp.) distribution and feeding habits of these species groups (Coyle & Pinchuk, 2005). Feeding habits of these species, like other zooplankton, are likely related to advection and water mass characteristics (Coyle, 2005; Walkusz, Storemark, & Skau, 2003).

The novel multi-trophic level Bayesian isotope mixing model presented here provides a new framework to evaluate trophic pathways and landscape connectivity in food webs. Unique to our model is a multi-species approach that incorporated data across trophic levels to inform shared parameters on source and tissue-specific discrimination. Thus we were able to use far more data than would be feasible with controlled laboratory studies alone. As the log-likelihood scales with sample size, using data from the whole food web afforded lower reliance on prior information to estimate the parameters of interest. Here we show this technique is a particularly effective tool for evaluating food web dynamics at the terrestrial-marine interface because of large gradients in ^{2}H between freshwater and marine sources.

Climate warming is expected to result in earlier timing of peak discharge, flashy hydrographs and greater interannual variability in freshwater delivery to the coastal areas of the Gulf of Alaska (O'Neel et al., 2015). As glaciers diminish in size, land-to-ocean discharge will eventually decrease in many regions (Bliss et al., 2014). This transition from glacial to non-glacial watersheds will increase the importance of rainfall as a hydrologic driver such that the delivery of riverine OM subsidies to marine ecosystems will become less regular and more event driven. Taxa with lower assimilation of riverine subsidies will likely be more capable of adapting to changing conditions. The effects of greater variability in the availability of allochthonous resources on species with substantial dependence on terrigenous subsidies will depend on their ability readily alter their exploitation of local resources. All the species examined in this study are capable of subsisting on in situ marine resources, assuming they are available. We anticipate, however, that ice-associated species like Kittlitz's murrelets in the Gulf of Alaska, which depend on glacier ice for nesting and are adapted to feeding conditions in the turbid glacier plumes (Arimitsu et al., 2012) will be most negatively affected by changes in delivery and timing of glacial runoff to coastal habitats.

ACKNOWLEDGEMENTS

Funding support was provided by U.S. Geological Survey Alaska Science Center and the North Pacific Research Board project 1206. We thank B. Heflin, J. King, E. Madison, S. Schoen, P. Raymond for help in the field or study design. We appreciate F. Mueter, A. Beaudreau, V. von Biela, V. Padula and two anonymous reviewers who provided insightful comments that improved this manuscript. All field procedures involving vertebrates were approved by University of Alaska Fairbanks IACUC (Assurance # 469319-3) and U.S. Geological Survey ACUC (Assurance # 2012-6). Any use of trade, firm, or product names is for descriptive purposes only and does not imply endorsement by the U.S. Government.

ORCID

Mayumi L. Arimitsu http://orcid.org/0000-0001-6982-2238
John F. Piatt http://orcid.org/0000-0002-4417-5748

REFERENCES

Abookire, A. A., Piatt, J. F., & Speckman, S. G. (2002). A nearsurface, daytime occurrence of two mesopelagic fish species (*Stenobrachius leucopsarus* and *Leuroglossus schmidti*) in a glacial fjord. *Fishery Bulletin*, *100*, 376–380.

Arendt, A., Walsh, J., & Harrison, W. (2009). Changes of glaciers and climate in northwestern North America during the late twentieth century. *Journal of Climate*, *22*, 4117–4134.

Arimitsu, M. L., Piatt, J. F., Litzow, M. A., Abookire, A. A., Romano, M. D., & Robards, M. D. (2008). Distribution and spawning dynamics of capelin (*Mallotus villosus*) in Glacier Bay, Alaska: A cold water refugium. *Fisheries Oceanography*, *17*, 137–146.

Arimitsu, M. L., Piatt, J. F., Madison, E. N., Conaway, J. S., & Hillgruber, N. (2012). Oceanographic gradients and seabird prey community dynamics in glacial fjords. *Fisheries Oceanography*, *21*, 148–169.

Arimitsu, M. L., Piatt, J. F., & Mueter, F. J. (2016). Influence of glacier runoff on ecosystem structure in Gulf of Alaska fjords. *Marine Ecology Progress Series*, *560*, 19–40.

Arimitsu, M. L., Piatt, J. F., Romano, M. D., Madison, E. N., & Conaway, J. S. (2010). Kittlitz's and marbled murrelets in Kenai Fjords National Park, south-central Alaska: At-sea distribution, abundance, and foraging habitat, 2006–08. USGS OFR 2010-1181.

Bardgett, R. D., Richter, A., Bol, R., Garnett, M. H., Bäumler, R., Xu, X., … Wanek, W. (2007). Heterotrophic microbial communities use ancient carbon following glacial retreat. *Biology Letters*, *3*, 487–490.

Batt, R. D., Carpenter, S. R., Cole, J. J., Pace, M. L., Johnson, R. A., Kurtzweil, J. R., & Wilkinson, G. M. (2015). Altered energy flow in the food web of an experimentally darkened lake. *Ecosphere*, *6*, 1–23.

Bliss, A., Hock, R., & Radić, V. (2014). Global response of glacier runoff to twenty-first century climate change. *Journal of Geophysical Research: Earth Surface*, *119*, 717–730.

Bustamante, R. H., & Branch, G. M. (1996). The dependence of intertidal consumers on kelp-derived organic matter on the west coast of South Africa. *Journal of Experimental Marine Biology and Ecology*, *196*, 1–28.

Caraco, N., Bauer, J. E., Cole, J. J., Petsch, S., & Raymond, P. A. (2010). Millennial-aged organic carbon subsidies to a modern river food web. *Ecology*, *91*, 2385–2393.

Caut, S., Angulo, E., & Courchamp, F. (2009). Variation in discrimination factors (Δ^{15}N and Δ^{13}C): The effect of diet isotopic values and applications for diet reconstruction. *Journal of Applied Ecology*, *46*, 443–453.

Coyle, K. O. (2005). Zooplankton distribution, abundance and biomass relative to water masses in eastern and central Aleutian Island passes. *Fisheries Oceanography*, *14*, 77–92.

Coyle, K. O., & Pinchuk, A. I. (2005). Seasonal cross-shelf distribution of major zooplankton taxa on the northern Gulf of Alaska shelf relative to water mass properties, species depth preferences and vertical migration behavior. *Deep-Sea Research II*, *52*, 217–245.

Cressie, N. (1988). Spatial prediction and ordinary kriging. *Mathematical Geology*, *20*, 405–421.

Diggle, P. J., & Ribeiro, P. J. Jr (2007). *Model-based geostatistics* (p. 228). New York: Springer.

Doucett, R. R., Marks, J. C., Blinn, D. W., Caron, M., & Hungate, B. A. (2007). Measuring terrestrial subsidies to aquatic food webs using stable isotopes of hydrogen. *Ecology*, *88*, 1587–1592.

Druffel, E. R. M., Williams, P. M., Bauer, J. E., & Ertel, J. R. (1992). Cycling of dissolved and particulate organic matter in the open ocean. *Journal of Geophysical Research*, *97*, 15639–15659.

Dunton, K. H., Saupe, S. M., Golikov, A. N., Schell, D. M., & Schonberg, S. V. (1989). Trophic relationships and isotopic gradients among arctic and subarctic marine fauna. *Marine Ecology Progress Series*, *56*, 89–97.

Erhardt, E. B., Wolf, B. O., Ben-David, M., & Bedrick, E. J. (2014). Stable isotope sourcing using sampling. *Open Journal of Ecology*, *4*, 289–298.

Fellman, J. B., Hood, E. W., Raymond, P. A., Hudson, J., Bozeman, M., & Arimitsu, M. L. (2015). Evidence for the assimilation of ancient glacier organic carbon in a proglacial stream food web. *Limnology and Oceanography*, *60*, 1118–1128.

Fellman, J. B., Spencer, R. G. M., Hernes, P. J., Edwards, R. T., D'Amore, D. V., & Hood, E. W. (2010). The impact of glacier runoff on the biodegradability and biochemical composition of terrigenous dissolved organic matter in near-shore marine ecosystems. *Marine Chemistry*, *121*, 112–122.

Finlay, J. C., Doucett, R. R., & McNeely, C. (2010). Tracing energy flow in stream food webs using stable isotopes of hydrogen. *Freshwater Biology*, *55*, 941–951.

Gearing, J. N. (1988). The use of stable isotope ratios for tracing the near-shore-offshore exhange of organic matter. In B. Jansson (Ed.), *Coastal-offshore ecosystem interactions* (pp. 69–101). Berlin: Springer-Verlag.

Guillemette, F., Bianchi, T. S., & Spencer, R. G. M. (2017). Old before your time: Ancient carbon incorporation in contemporary aquatic foodwebs. *Limnology and Oceanography*, *62*, 1682–1700.

Hågvar, S., & Ohlson, M. (2013). Ancient carbon from a melting glacier gives high ^{14}C age in living pioneer invertebrates. *Scientific Reports*, *3*, 2820. https://www.nature.com/articles/srep02820?WT.ec_id=SREP-631-20131101

Hatch, S. A., Robertson, G. J., & Baird, P. H. (2009). Black-legged Kittiwakes (*Rissa tridactyla*). In P. G. Rodewald (Ed.), *Birds of North America Online*. Cornell Lab of Ornithology: Ithaca.

Hedges, J. I., Keil, R. G., & Benner, R. (1997). What happens to terrestrial organic matter in the ocean? *Organic Geochemistry*, *27*, 195–212.

Hill, D. F., Bruhis, N., Calos, S. E., Arendt, A. A., & Beamer, J. (2015). Spatial and temporal variability of freshwater discharge into the Gulf of Alaska. *Journal of Geophysical Research: Oceans*, *120*, 634–646.

Hobson, K. A. (1990). Stable isotope analysis of Marbled Murrelets: Evidence for freshwater feeding and determination of trophic level. *The Condor*, *92*, 897–903.

Hobson, K. A. (1993). Trophic relationsips among high Arctic seabirds: Insights from tissue-dependent stable-isotope models. *Marine Ecology Progress Series*, *95*, 7–18.

Hobson, K. A., Piatt, J. F., & Pitocchelli, J. (1994). Using stable isotopes to determine seabird trophic relationships. *Journal of Animal Ecology*, *63*, 786–798.

Hoffman, M. D., & Gelman, A. (2014). The No-U-turn sampler: Adaptively setting path lengths in Hamiltonian Monte Carlo. *The Journal of Machine Learning Research*, *15*(1), 1593–1623.

Hood, E. W., Fellman, J. B., Spencer, R. G. M., Hernes, P. J., Edwards, R., D'Amore, D. V., & Scott, D. (2009). Glaciers as a source of ancient and labile organic matter to the marine environment. *Nature*, *462*, 1044–1047.

Iverson, S. J., Frost, K. J., & Lang, S. (2002). Fat content and fatty acid composition of forage fish and invertebrates in Prince William Sound, Alaska: Factors contributing to among and within species variability. *Marine Ecology Progress Series*, *241*, 161–181.

Kissling, M. L., Lukacs, P. M., Gende, S. M., & Lewis, S. B. (2015). Multistate mark-recapture model to estimate survival of a dispersed-nesting seabird, the Kittlitz's Murrelet. *Journal of Wildlife Management*, *79*, 20–30.

Kline, T. C. Jr. (2009). Characterization of carbon and nitrogen stable isotope gradients in the northern Gulf of Alaska using terminal feed stage copepodite-V *Neocalanus cristatus*. *Deep-Sea Research Part II*, *56*, 2537–2552.

Kruschke, J. K. (2013). Bayesian estimation supersedes the t test. *Journal of Experimental Psychology: General*, *142*, 573–603.

Ladd, C., Hunt, G. L., Mordy, C. W., Salo, S. A., & Stabeno, P. J. (2005). Marine environment of the eastern and central Aleutian Islands. *Fisheries Oceanography*, *14*, 22–38.

Larsen, C. F., Burgess, E., Arendt, A. A., O'Neel, S., Johnson, A. J., & Lienholz, C. (2015). Surface melt dominates Alaska glacier mass balance. *Geophysical Research Letters*, *42*, 5902–5908.

Lis, G., Wassenaar, L. I., & Hendry, M. J. (2008). High-precision laser spectroscopy D/H and ^{18}O/^{16}O measurements of microliter natural water samples. *Analytical chemistry*, *80*, 287–293.

Lydersen, C., Assmy, P., Falk-Petersen, S., Kohler, J., Kovacs, K. M., Reigstad, M., … Zajaczkowskic, M. (2014). The importance of tidewater glaciers for marine mammals and seabirds in Svalbard, Norway. *Journal of Marine Systems*, *129*, 452–471.

Mizutani, H., Kabaya, Y., & Wada, E. (1991). Nitrogen and carbon isotope compositions relate linearly in cormorant tissues and its diet. *Isotopenpraxis*, *27*, 166–168.

Neal, E. G., Hood, E. W., & Smikrud, K. (2010). Contribution of glacier runoff to freshwater discharge into the Gulf of Alaska. *Geophysical Research Letters*, *37*, L06404. http://onlinelibrary.wiley.com/doi/10.1029/2010GL042385/full

Niebauer, H. J., Royer, T. C., & Weingartner, T. J. (1994). Circulation of Prince William Sound, Alaska. *Journal of Geophysical Research*, *99*, 14113–14126.

O'Neel, S., Hood, E., Bidlack, A. L., Fleming, S. W., Arimitsu, M. L., Arendt, A., … Pyare, S. (2015). Icefield-to-ocean linkages across the Northern Pacific coastal temperate rainforest ecosystem. *BioScience*, *65*, 499–512.

Ostrom, P. H., Wiley, A. E., Rossman, S., Stricker, C. A., & James, H. F. (2014). Unexpected hydrogen isotope variation in oceanic pelagic seabirds. *Oecologia*, *175*, 1227–1235.

Pfeffer, W. T., Arendt, A. A., Bliss, A., Bolch, T., Cogley, J. G., Gardner, A. S., ... The Randolph Consortium (2014). The Randolph Glacier Inventory: A globally complete inventory of glaciers. *Journal of Glaciology*, *60*, 537–552.

Piwosz, K., Walkusz, W., Hapter, R., Wieczorek, P., Hop, H., & Wiktor, J. (2009). Comparison of productivity and phytoplankton in a warm (Kongsfjorden) and a cold (Hornsund) Spitsbergen fjord in mid-summer 2002. *Polar Biology*, *32*, 549–559.

Post, D. M. (2002). Using stable isotopes to estimate trophic position: Models, methods, and assumptions. *Ecology*, *83*, 703–718.

Quillfeldt, P., Bugoni, L., McGill, R. A. R., Masello, J. F., & Furness, R. W. (2008). Differences in stable isotopes in blood and feathers of seabirds are consistent across species, age and latitude: Implications for food web studies. *Marine Biology*, *155*, 593–598.

R Core Team. (2017). *A language and environment for statistical computing*. Vienna, Austria: R Foundation for Statistical Computing. https://www.R-project.org/.

Raymond, P. A., & Bauer, J. E. (2001). Use of ^{14}C and ^{13}C natural abundances for evaluating riverine, estuarine, and coastal DOC and POC sources and cycling: A review and synthesis. *Organic Geochemistry*, *32*, 469–485.

Ribeiro, P. J. Jr., & Diggle, P. J. (2015). geoR: Analysis of geostatistical data. R package version 1.7-5.1. http://CRAN.R-project.org/package=geoR.

Schell, D. M. (1983). Carbon-13 and Carbon-14 abundances in Alaskan aquatic organisms: Delayed production from peat in Arctic food webs. *Science*, *219*, 1068–1071.

Schell, D. M., Barnett, B., & Vinette, K. (1998). Carbon and nitrogen isotope ratios in zooplankton of the Bering, Chukchi and Beaufort seas. *Marine Ecology Progress Series*, *162*, 11–23.

Schoen, S. K., Piatt, J. F., Arimitsu, M. L., Madison, E., Drew, G., Renner, M., & Heflin, B. (2014). *Seabirds as marine ecosystem indicators across the Aleutian Archipelago*. USGS report. Anchorage, AK. 27 pp.

Sessions, A. L., Burgoyne, T. W., Schimmelmann, A., & Hayes, J. M. (1999). Fractionation of hydrogen isotopes in lipid biosynthesis. *Organic Geochemistry*, *30*, 1193–1200.

Singer, G. A., Fasching, C., Wilhelm, L., Niggemann, J., Steier, P., Dittmar, T., & Battin, T. J. (2012). Biochemically diverse organic matter in Alpine glaciers and its downstream fate. *Nature Geoscience*, *5*, 710–714.

Solomon, C. T., Carpenter, S. R., Clayton, M. K., Cole, J. J., Coloso, J. J., Pace, M. L., ... Weidel, B. C. (2011). Terrestrial, benthic, and pelagic resource use in lakes: Results from a three-isotope Bayesian mixing model. *Ecology*, *92*, 1115–1125.

Solomon, C. T., Cole, J. J., Doucett, R. R., Pace, M. L., Preston, N. D., Smith, L. E., & Weidel, B. C. (2009). The influence of environmental water on the hydrogen stable isotope ratio in aquatic consumers. *Oecologia*, *161*, 313–324.

Soto, D. X., Wassenaar, L. I., & Hobson, K. A. (2013). Stable hydrogen and oxygen isotopes in aquatic food webs are tracers of diet and provenance. *Functional Ecology*, *27*, 535–543.

Soto, D. X., Wassenaar, L. I., Hobson, K. A., Catalan, J., & Trudel, M. (2011). Effects of size and diet on stable hydrogen isotope values (δD) in fish: Implications for tracing origins of individuals and their food sources. *Canadian Journal of Fisheries and Aquatic Sciences*, *68*, 2011–2019.

Sprules, W. G., & Bowerman, J. E. (1988). Omnivory and food chain length in zooplankton food webs. *Ecology*, *69*, 418–426.

Stan Development Team. (2016). Stan: A C++ library for probability and sampling, Version 2.9.0-3.

Vander Zanden, M. J., & Rasmussen, J. B. (2001). Variation in δ15N and δ13C trophic fractionation: Implications for aquatic food web studies. *Limnology and Oceanography*, *46*, 2061–2066.

Vander Zanden, H. B., Soto, D. X., Bowen, G. J., & Hobson, K. A. (2016). Expanding the isotopic toolbox: Applications of hydrogen and oxygen stable isotope ratios to food web studies. *Frontiers in Ecology and Evolution*, *4*, 1–19.

Vargas, C. A., Martinez, R. A., San Martin, V., Aguayo, M., Silva, N., & Torres, R. (2011). Allochthonous subsidies of organic matter across a lake-river-fjord landscape in the Chilean Patagonia: Implications for marine zooplankton in inner fjord areas. *Continental Shelf Research*, *31*, 187–201.

Walinsky, S. E. E., Prahl, F. G., Mix, A. C. C., Finney, B. P. P., Jaeger, J. M. M., & Rosen, G. P. P. (2009). Distribution and composition of organic matter in surface sediments of coastal Southeast Alaska. *Continental Shelf Research*, *29*, 1565–1579.

Walkusz, W., Storemark, K., & Skau, T. (2003). Zooplankton community structure; a comparison of fjords, open water and ice stations in the Svalbard area. *Polish Polar Research*, *24*, 149–165.

Wassenaar, L. I., & Hobson, K. A. (2003). Comparative equilibration and online technique for determination of non-exchangeable hydrogen of keratins for use in animal migration studies. *Isotopes in Environmental and Health Studies*, *39*, 211–217.

Weingartner, T. J., Danielson, S. L., & Royer, T. C. (2005). Freshwater variability and predictability in the Alaska Coastal Current. *Deep Sea Research Part II*, *52*, 169–191.

Whitworth, D. L., Takekawa, J. Y., Carter, H. R., & McIver, W. R. (1997). A night-lighting technique for at-sea capture of Xantus' Murrelets. *Colonial Waterbirds*, *20*, 525–531.

Wilkinson, G. M., Cole, J. J., & Pace, M. L. (2015). Deuterium as a food source tracer: Sensitivity to environmental water, lipid content, and hydrogen exchange. *Limnology and Oceanography: Methods*, *13*, 213–223.

Witteveen, B. H. (2011). Trophic levels of north Pacific humpback whales (*Megaptera novaeangliae*) through analysis of stable isotopes: Implications on prey and resource quality. *Aquatic Mammals*, *37*, 101–110.

Wu, J., Calvert, S. E., Wong, C. S., & Whitney, F. A. (1999). Carbon and nitrogen isotopic composition of sedimenting particulate material at Station Papa in the subarctic northeast Pacific. *Deep-Sea Research Part II*, *46*, 2793–2832.

Yang, C., Wilkinson, G. M., Cole, J. J., Macko, S., & Pace, M. (2014). Assigning hydrogen, carbon, and nitrogen isotope values for phytoplankton and terrestrial detritus in aquatic food web studies. *Inland Waters*, *4*, 233–242.

Yodzis, P. (1984). Energy flow and the vertical structure of real ecosystems. *Oecologia*, *65*, 86–88.

SUPPORTING INFORMATION

Additional Supporting Information may be found online in the supporting information tab for this article.

How to cite this article: Arimitsu ML, Hobson KA, Webber DN, Piatt JF, Hood EW, Fellman JB. Tracing biogeochemical subsidies from glacier runoff into Alaska's coastal marine food webs. *Glob Change Biol*. 2018;24:387–398. https://doi.org/10.1111/gcb.13875